HST Spectroscopy of Lyα Emission in Low-Redshift Weak Emission-Line Quasars: Implications for Rapid Accretion in Active Galactic Nuclei

Jeremiah D. Paul[1], Richard M. Plotkin[1], Ohad Shemmer[2], Scott F. Anderson[3], W. N. Brandt[4], Xiaohui Fan[5], Bin Luo[6], Qingling Ni[7,4], Donald P. Schneider[4], Jianfeng Wu[8], Weimin Yi[9,4]

1. University of Nevada, Reno, NV, USA. 2. University of North Texas, Denton, TX, USA. 3. University of Washington, Seattle, WA, USA. 4. Pennsylvania State University, University Park, PA, USA. 5. University of Arizona, Tucson, AZ, USA. 6. Nanjing University, Nanjing, Jiangsu, China. 7. University of Edinburgh, Edinburgh, UK. 8. Xiamen University, Xiamen, Fujian, China. 9. Yunnan Observatories, Kunming, Yunnan, China.

Introduction

Type 1 radio-quiet quasars (QSOs) display complex spectra with signatures of interaction between the radiative processes of multiple distinct physical regions. Broad line region (BLR) gas orbits deep within the gravitational potential well of the QSO's central black hole and reprocesses incident X-ray and ultraviolet (UV) radiation into strong, broad (FWHM $> 10^3$ km s^{-1}) emission lines in optical-UV rest-frame wavebands.[1] However, puzzling examples of QSOs with intrinsically weak or absent broad emission lines (Fig. 1) have been found.[2] Studies have suggested that the BLR in these objects is either poorly ionized or gas deficient (illustrated at right),[3,4,5,6] but a singular cause has yet to be determined.

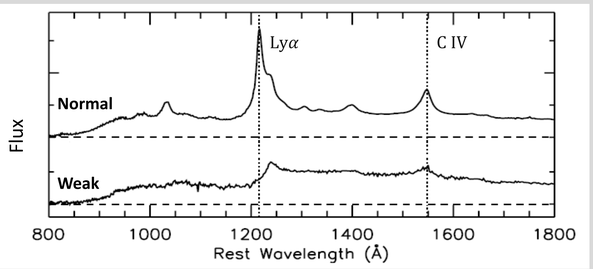

Figure 1: Composite spectra comparing "normal" and "weak-lined" quasars. Adapted from Diamond-Stanic et al. (2009).[71]

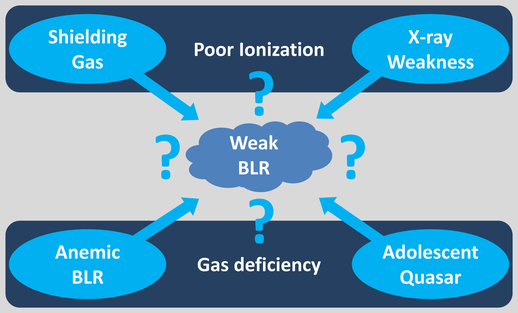

The first systematic searches for these weak emission-line QSOs (WLQs) investigated the rest-frame equivalent width (EW) of the Lyα + Nv complex and revealed a high-redshift ($z > 3$) population, defined by a 3σ-weak threshold of EW[Lyα+Nv] $<$ 15.4 Å.[7] Identification of lower-redshift ($z < 3$) WLQ candidates, however, has relied on weak broad emission lines at longer rest-frame wavelengths. This disparity between identification standards must be broken to unify the populations and determine how WLQs relate to QSO evolution.

Methods

We undertook a pilot study to expand waveband coverage of suspected low-z ($z < 3$) WLQs in order to better understand the shapes of their ionizing continua and explore unification of the low- and high-z populations through the Lyα EW diagnostic. We selected 6 moderately low-redshift ($0.9 < z < 1.5$) candidate WLQs with existing X-ray (Chandra) and optical (SDSS) coverage and obtained new Hubble Space Telescope (HST) UV spectra covering the Lyα + Nv emission range (Fig. 2).

For each candidate, we fit a model broken power law continuum and recorded the continuum slopes via the power law spectral indices $\alpha_{\rm FUV}$ (blueward of the break) and $\alpha_{\rm NUV}$ (redward). The break typically fell at $\sim$1000 − 1200 Å. We then fit a local linear continuum to the Lyα + Nv emission range and measured EW[Lyα+Nv] via integration of the normalized observed flux. To facilitate evaluation of our targets' ionizing continua, we also retrieved X-ray flux and broad-line Mg II λ2800 EW measurements from the literature.[5,6,9] Values are reported in Table 1 below.

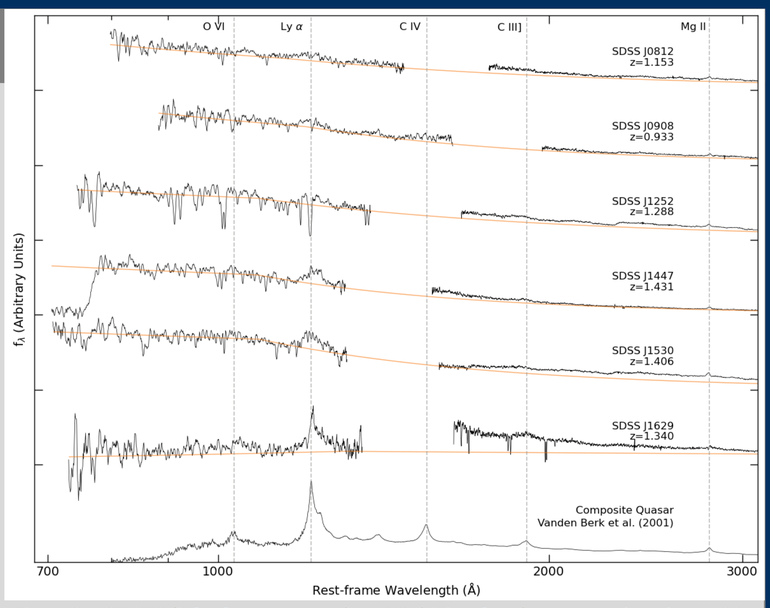

Figure 2: HST STIS (left of coverage gap) + SDSS (right of gap) spectra redward to 3100 Å of all six WLQ candidates (object names, truncated here to the first 4 digits, are given in full in Table 1 below), along with the QSO composite from Vanden Berk et al. (2001). Observed flux density (vertical, arbitrary units/scaling) vs. rest-frame wavelength (horizontal, Å in log scale) is shown in black; model broken power law continuum in orange. Vertical dashed lines show rest-frame positions of several prominent QSO emission lines.

Results & Discussion

Two of our targets unify well WLQs, with EW[Lyα+Nv] $<$ 15.4 Å. Three others are consistent with a "bridge" population,[10] with EW[Lyα+Nv] above the 3σ-weak threshold but still near or below the 2σ-weak (24.7 Å) threshold.[7] The final target appears heavily absorbed in UV, but still has EW[Lyα+Nv] typical of "normal" QSOs and is eliminated as a candidate. **Our WLQs and bridge QSOs span a range of X-ray weakness that is not correlated with their EW[Lyα+Nv] (Fig. 3), likely ruling out intrinsic X-ray weakness as the primary cause of weak BLR emission.**

Furthermore, the range of EW[Lyα+Nv] to EW[MgII] ratios displayed by our targets indicates that while both lines appear weak in WLQs, Lyα ($\chi_{\rm ion} = 13.6$ eV) is *preferentially* weakened over Mg II ($\chi_{\rm ion} = 7.6$ eV). Even so, our WLQs and bridge QSOs have HST UV spectral slopes ($\alpha_{\rm FUV}$ and $\alpha_{\rm NUV}$) generally typical of "normal" QSOs.[8,11] **These results are consistent with a "slim disk" model in which rapid (i.e., near/super-Eddington) accretion causes the innermost radii of the disk to swell and shield the BLR from ionizing X-ray and extreme UV radiation (Fig 4).**[5,6,10]

Source Name (SDSS J) [a]	z [b]	$\Delta\alpha_{\rm ox}$ [c]	$\alpha_{\rm FUV}$ [d]	$\alpha_{\rm NUV}$ [e]	EW[Lyα+Nv] (Å) [f]	EW[MgII] (Å) [g]
081250.80 + 522530.8	1.153	-0.41	-1.0 ± 0.2	$-1.4^{+0.3}_{-0.1}$	15.3 ± 2.3	8.4 ± 0.7
090843.25 + 285229.8	0.933	0.11	$-1.0^{+0.4}_{-0.3}$	$-2.0^{+0.3}_{-0.2}$	10.7 ± 2.3	7.8 ± 1.0
125219.48 + 264053.9	1.288	-0.39	-0.5 ± 0.2	-1.5 ± 0.2	21.9 ± 2.7	8.7 ± 0.4
144741.7 − 020339.1	1.431	-0.13	-0.5 ± 0.1	-2.2 ± 0.2	26.4 ± 3.0	12.1 ± 0.7
153044.08 + 231013.5	1.406	0.22	$-0.3^{+0.2}_{-0.1}$	-2.0 ± 0.2	28.3 ± 3.2	12.9 ± 0.4
162933.60 + 253200.6	1.340	-0.03	$+0.9^{+0.8}_{-1.4}$	-1.6 ± 0.1	83.7 ± 18.6	12.3 ± 0.1

Table 1: (a) Object name. (b) Redshift. (c) X-ray weakness represented by the ratio $l_{\rm 2keV}/l_{\rm 2500Å}$ (respectively, the specific luminosities at 2 keV and 2500 Å)[5,6] emitted relative to the expectation for a "normal" broad-line QSO at comparable $l_{\rm 2500Å}$.[12] More negative values are more X-ray weak. (d) Our measured UV spectral index blueward of power law model break. (e) Our measured UV spectral index redward of power law model break. (f) Our measured EW for the Lyα + Nv complex. (g) EW for Mg II λ2800 obtained from Shen et al. 2011.[9]

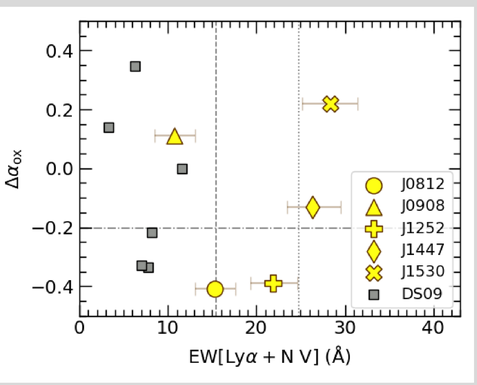

Figure 3 (Left): Comparison of Lyα emission strength (horizontal axis) to X-ray weakness (vertical axis). X-ray weakness is given by $\Delta\alpha_{\rm ox}$ (see Table 1 notes). Yellow symbols represent our targets, and grey dots show a small sample of high-z WLQs from Diamond-Stanic et al. (2009) with X-ray fluxes in the literature.[4,7] The horizontal dash-dot line gives the conventional threshold below which an object is considered "X-ray weak." The vertical dashed and dotted lines respectively give the 3σ- and 2σ-weak thresholds for EW[Lyα+Nv].[7] ***A Pearson correlation test shows no correlation between $\Delta\alpha_{ox}$ and EW[Lyα+Nv] in this sample ($r = -0.17; p = 0.84$).***

Figure 4 (Right): Diagram depicting the cross-section of a slim accretion disk model. The BLR is shielded from ionizing radiation by the inner edges of the disk, while the observed X-ray flux is dependent on orientation. Adapted from Ni et al. (2018).[10]

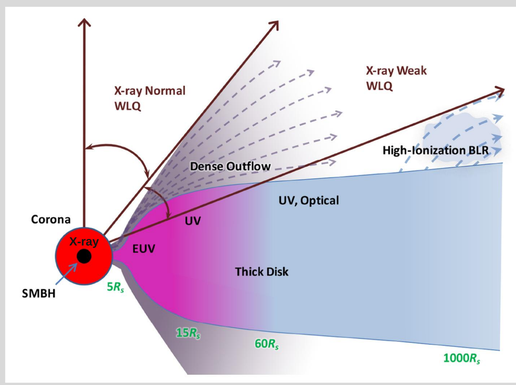

Future Work

A perplexing X-ray weak tail has been observed in lower-mass ($M_{\rm BH} \sim 10^6 M_\odot$), rapidly-accreting, radio-quiet active galactic nuclei (AGNs; see Fig. 5).[13] It may be that these objects also possess slim accretion disks and that we observe orientation-dependent X-ray shielding. For a sample of these AGNs, we will combine new and archival radio observations from the Very Large Array (VLA) with archival X-ray observations from Chandra.

In radio-quiet AGNs, correlations found between radio and X-ray luminosities indicate they share a common driver.[14] Moreover, the radio emission should originate outside potential shielding zones and is therefore expected to be isotropic even when X-ray obscuration is present. **If X-ray weakness in our VLA sample is intrinsic (e.g., due to weak disk-corona coupling), we should see a constant ratio of radio to X-ray luminosities. If it is orientation-induced, the ratio should scale in relation to the X-ray weakness.** This experiment may be applicable to radio-quiet AGNs across mass/evolutionary populations, including WLQs.

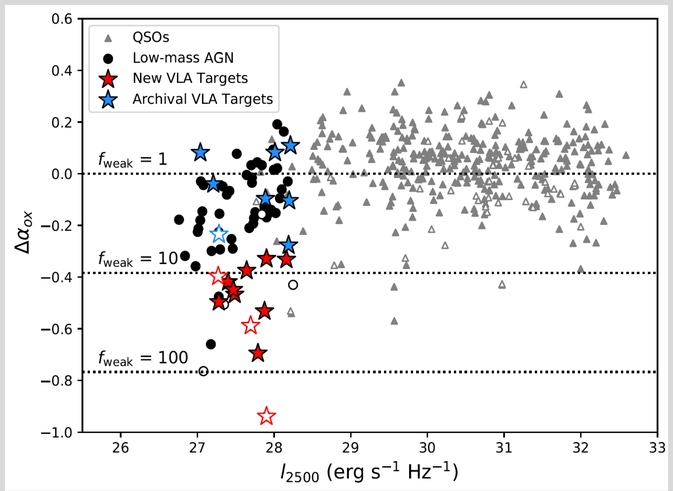

Figure 5: X-ray weakness ($\Delta\alpha_{\rm ox}$) vs. specific luminosity at 2500 Å ($l_{\rm 2500Å}$). Black circles show low-mass AGN, with our VLA sample represented by blue and red stars (see legend). Grey triangles represent ~370 "normal" broad-line QSOs from Just et al. (2007).[12] All open symbols represent X-ray non-detections. Horizontal dotted lines show a derived X-ray weakness factor. ***Note the distinct X-ray weak tail for low-mass AGN.*** Adapted from Plotkin et al. (2016).[13]

References

1. Osterbrock & Mathews 1986, ARA&A, 24, 171.
2. Fan et al. 1999, ApJL, 526, L57.
3. Leighly et al. 2007, ApJ, 663, 103.
4. Shemmer et al. 2009, ApJ, 696, 580.
5. Wu et al. 2012, ApJ, 747, 10.
6. Luo et al. 2015, ApJ, 805, 122.
7. Diamond-Stanic et al. 2009, ApJ, 699, 782.
8. Telfer et al. 2002, ApJ, 565, 773.
9. Shen et al. 2011, ApJS, 194, 45.
10. Ni et al. 2018, MNRAS, 480, 5184.
11. Vanden Berk et al. 2001, AJ, 122, 549.
12. Just et al. 2007, ApJ, 665, 1004.
13. Plotkin et al. 2016, ApJ, 825, 139.
14. Panessa et al. 2015, MNRAS, 447, 1289.